Control of brain state transitions with light

Almudena Barbero[a,†], Fabio Riefolo[b,c,†], Carlo Matera[b,c], Enrique Claro[d], Maria Victoria Sánchez-Vives[a,e,*], and Pau Gorostiza[b,c,e,*]

a. Hospital Clínic; University of Barcelona (UB); IDIBAPS.

b. Institute for Bioengineering of Catalonia (IBEC), Barcelona Institute for Science and Technology (BIST).

c. Network Biomedical Research Center in Bioengineering, Biomaterials, and Nanomedicine (CIBER-BBN).

d. Institut de Neurociències and Departament de Bioquímica i Biologia Molecular, Unitat de Bioquímica de Medicina, Universitat Autònoma de Barcelona (UAB).

e. Catalan Institution for Research and Advanced Studies (ICREA).

† Equivalent contribution.

* Corresponding authors. E-mail: msanche3@clinic.cat (M.V. S.-V.), pau@icrea.cat (P. G.)

ABSTRACT

Human behavior is driven by specific neuronal activity and can be directly associated to characteristic brain states. The oscillatory activity of neurons contains information about the mental state of an individual, and the transition between different brain states is controlled by the neuromodulatory action of acetylcholine on nicotinic and muscarinic receptors. Manipulating brain waves bears high therapeutic interest in several neurological disorders, and can be achieved by transcranial direct current and magnetic stimulation techniques, and by optogenetics, although the clinical translation of the latter is hampered by the need of gene therapy. Here, we directly modulate brain waves with light using a photoswitchable muscarinic agonist. Synchronous slow wave activity can be disrupted in isolated cortical slices and in anesthetized mice. These results open the way to study the spatiotemporal distribution and the pharmacology of brain states, their transitions, and their links to cognition and behavior, in a diversity of wildtype organisms.

INTRODUCTION

All behaviors, thoughts, and emotions are rooted in the communication between the billions of neurons that constitute the brain.[1–3] Individual neurons transmit information using chemical and electrical signals, and are organized in groups or "circuits" that carry out a certain function.[3–5] The electro-chemical interactions of these groups of neurons produce synchronized electrical activity in the brain, called "brain waves" due to their periodic and propagating properties.[6–8] They can be recorded by electroencephalography (EEG), and local field potential (LFP) measurements. Brain waves, their frequency and other characteristic parameters, are associated to internal brain states and result in specific behaviors.[1] The entirety of neuronal activity undergoes important changes during brain and behavioral state transitions, which have been linked to strong changes in the EEG pattern activity.[9] For example, large and synchronous brainwaves are mostly associated with deep sleep, whereas wakefulness shifts them toward more desynchronized and short-amplitude wave patterns.[7,10,11] These changes in brain and behavioral states, and the concomitant alterations in EEG activity, can be driven by the action of neuromodulators like acetylcholine (ACh).[9,12]

However, it is not known how the different cells expressing ACh receptors contribute to altering the global cortical state. Cholinergic receptors include nicotinic ion channels and muscarinic G protein-coupled receptors. Together, they modulate cortical activity on a fine spatial scale and are involved in crucial neocortical functions such as attention,[13,14] learning,[15–17] memory,[18] and sensory and motor functions.[19,20] In the neocortex, ACh is released mostly at cholinergic afferents from neurons distributed within the basal forebrain (BF) nuclei. Electrical stimulation of nucleus basalis can evoke the release of ACh in the neocortex but in an unselective manner, as ascending projections from BF nuclei not only comprise cholinergic axons, but also GABAergic and glutamatergic axons.[21] Such lack of selectivity complicates the study of cholinergic signaling in neocortex and its effects on controlling brain states.

Selective stimulation of cholinergic projections in the neocortex from BF nuclei has been demonstrated with optogenetics, which enables disrupting neocortical synchronous activity during certain sleep states. Optogenetic stimulation of BF cholinergic neurons also revealed their influence in awake cortical dynamics, coding properties of V1 neurons, and the importance of cholinergic neuromodulation for visual discrimination tasks, showing that stimulation of BF cholinergic cells activates cortical transitions faster than presumed.[10] However, the cell type specificity of optogenetics is limited by the availability of suitable promoters. In addition, it is based on the overexpression of microbial proteins using genetic manipulation, which raise safety and regulatory concerns when therapeutic applications are considered.

The control of neuronal signalling with photopharmacology is based on synthetic ligands that target endogenous proteins, and thus its physiological relevance spans from the circuits to the sub-cellular levels. For the same reason, photoswitchable ligands can generally be used in multiple species, and their safety and regulation can be established as for other drugs. Since the cholinergic system is key to modulate various CNS functions,[22] the use of selective and photoswitchable cholinergic drugs to spatiotemporally control cortical activity would have relevant scientific and clinical implications. Herein, we report that the cholinergic-dependent brain state transitions in the neocortex can be directly controlled using Phthalimide-Azo-Iper (PAI)[23] a photoswitchable agonist that targets M2 muscarinic acetylcholine receptors (mAChRs) without requiring electric or genetic manipulation. In particular, PAI enables modulating spontaneous emerging slow oscillations (SO) in neuronal circuits. PAI *cis*-to-*trans* photoisomerization decreases the Down- and Up-state durations, and increases the oscillatory frequency in cortical slices. In addition, PAI allows reversibly manipulating the cortical oscillation frequency in anesthetized mice using light. Thus, photopharmacology allows for the first time selectively controlling SO *in vitro* and *in vivo*, opening the way to dissect their spatiotemporal dynamics and their effects on brain and behavioural state transitions.

RESULTS

Non-specific activation of mAChRs evokes neuronal hyperexcitability in cortical slices

Alterations in cortical rhythms underlie behavioral state transitions, and neuronal ACh actions play central roles in such variations.[24–30] However, a complete and unifying view has not yet emerged[11] about the cholinergic impact on neuronal and synaptic physiology, and thus on neocortical network dynamics. It is known that ACh shifts the neocortical network state from a synchronous to asynchronous activity in a dose-dependent manner, but the activity of ACh on the vast majority of neocortical neurons and synapses is poorly characterized. Neocortical activation of mAChRs *in vitro* facilitates synaptic transmission,[31] recurrent excitation,[32] and reversibly increases the power of fast-frequency oscillations.[33–36] On this basis, we first studied *in vitro* the effect of Iperoxo, a potent muscarinic agonist.[37] The goal was to evaluate the potential of

mAChRs to selectively modulate the dynamics of isolated V1 cortical slices, while avoiding the simultaneous activation of nicotinic cholinergic receptors (nAChRs), and to validate Iperoxo photoswitches and useful photopharmacological tools to control neuronal activity. Isolated cortical slices spontaneously generate cortical SO, a hallmark of activity during deep sleep or anesthesia.[38] We recorded the spontaneous oscillatory activity (control) and then under different concentrations (1, 10, 100 nM) of Iperoxo. Slow wave activity alternates periods of activity or high neuronal firing (Up state) and periods of near silence (Down state). The activation of mAChRs by Iperoxo resulted in a global change in the network's dynamics to an hyperexcitable activity (**Fig. 1**). At 100 nM Iperoxo, the OF increased (from 0.89 ± 0.12 Hz in the control, to 1.34 ± 0.18 Hz with 100 nM Iperoxo), and the relative firing rate of the Up-states decreased (from 1.13 ± 0.23 a.u. to 0.10 ± 0.02 with 100 nM Iperoxo) (**Fig. 1B**). In addition, at concentrations equal or higher than 100 nM Iperoxo, the oscillatory activity evolved to periods of seizure-like discharges (**Fig.1C**),[39,40] characterized by low (<1 Hz), delta (1-4 Hz) and alfa (8-12 Hz) frequencies (**Fig. 1D**).

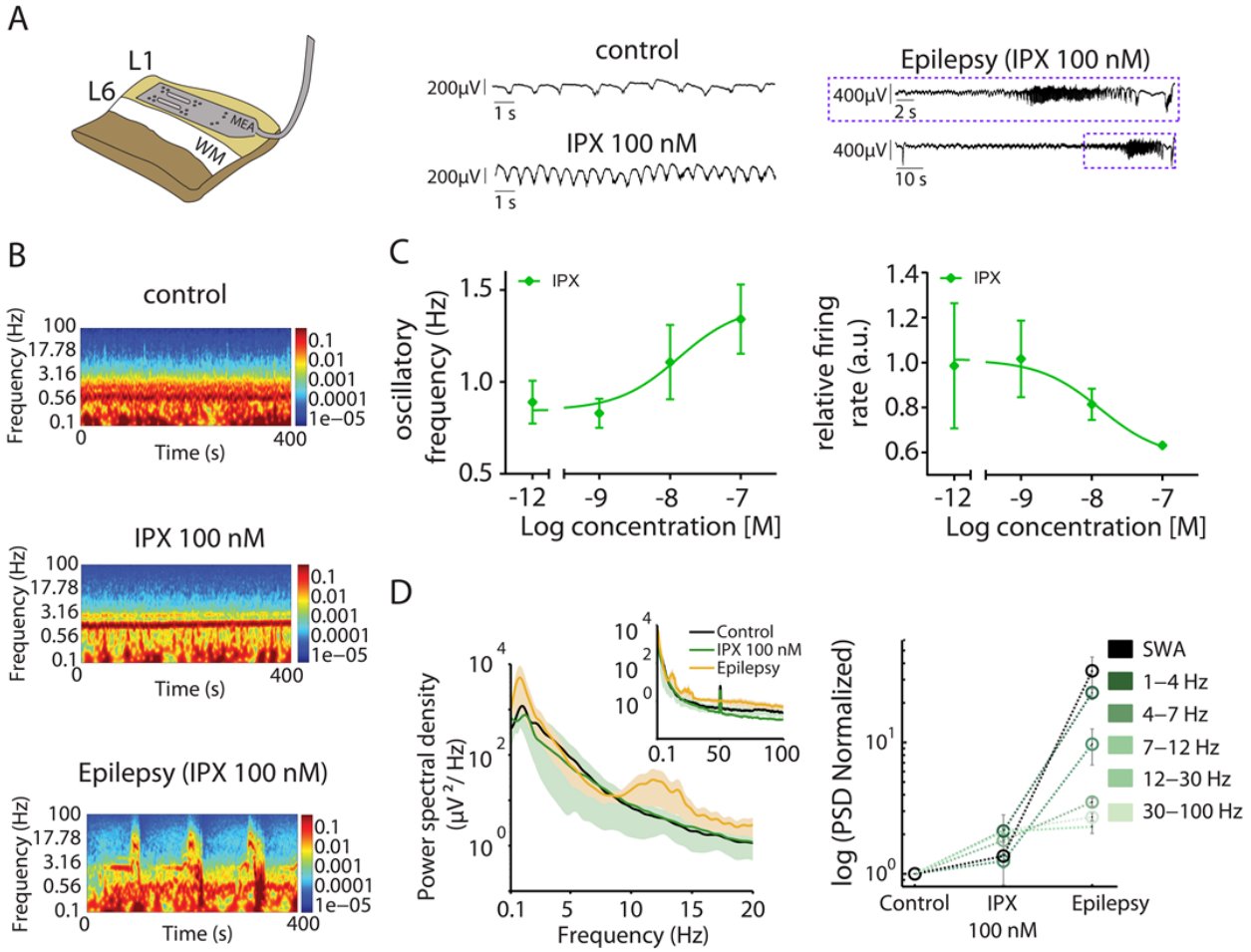

Figure 1: Non-specific activation of mAChRs evokes neuronal hyperexcitability in cortical slices. (**A**) On the left, the experimental setup: MEA, multielectrode array; WM, white matter; L1-L6, layer 1-6. On the right, representative Local Field Potential (LFP) traces showing the increasing of the OF corresponding to the Spectrogram of panel **B**. (**B**) Spectrogram under color from the same time recording of LFP traces on panel **A**: control, 100 nM Iperoxo and periods seizure - like discharges. (**C**) OF (Hz) and relative firing rate (a.u.). (**D**) Power spectral density (PSD) values showing low, delta and theta frequency component. Normalized PSD values at different frequency bands.

Effect of PAI isomers on slow and fast oscillations *in vitro*

The hyperexcitable activity obtained with Iperoxo reflects the role of mAChRs activation in cortical networks and brain states.[11] In order to remotely control these states, we aimed at the observed muscarinic

neuromodulation using PAI, a photoswitchable Iperoxo derivative that allows reversibly activating M2 mAChRs with light.[23] M2 receptors play relevant roles in several CNS disorders,[22] and regulating their activity and subsequent effects on cortical neuronal networks may provide new therapeutic opportunities for these cholinergic diseases.

Taking advantage of its profile as M2 light-regulated agonist, we studied its effect on the modulation of neuronal oscillations in cortical slices, as M2. Thus, we applied PAI and illumination to brain slices and recorded their oscillatory activity. We first built up the dose-response curves of the two drug forms separately, *trans*- (dark-adapted state) and *cis*-PAI (after UV irradiation), in order to find out the differences in cortical activity between the PAI-isoforms, and to identify the most convenient concentration range to manipulate brain waves with light. The baseline activity (characterized by SO) was recorded as a control, prior to bath-application of solutions with increasing PAI concentrations (10 nM, 100 nM, 300 nM, and 1 µM, n = 6 for each PAI form, *trans* and *cis*) (**Fig. 2A**). Comparing to the control situation, the *trans*-PAI activity showed alterations in the Up- and Down-state sequence already at 100 nM (**Fig.2**), leading an increment in the OF (from 0.58 ± 0.06 Hz during control to 1.87 ± 0.12 Hz applying 1 µM *trans*-PAI) (**Fig. 2B**). Moreover, increasing concentrations of *trans*-PAI decreased the relative firing rate during the Up states (from 0.98 ± 0.11 a.u. during control to 0.37 ± 0.03 a.u. with 1 µM *trans*-PAI) (**Fig. 2C, D).** In comparison, *cis*-PAI displayed significantly weaker effects, in agreement with the reported PAI properties.[23] At 100 nM and 300 nM, *cis*-PAI did not alter the spontaneous activity observed in control experiments (control OF: 0.48 ± 0.037 Hz; 100 nM *cis*-PAI OF: 0.52 ± 0.07 Hz; 300 nM *cis*-PAI OF: 0.87 ± 0.2 Hz), in contrast to the strong alterations in oscillatory activity obtained with 100 nM and 300 nM *trans*-PAI (**Fig. 2**). Only at concentrations as high as 1 µM, *cis*-PAI altered the Up- and Down-state sequence in comparison to the control, increasing the OF (1.32 ± 0.27Hz) and decreasing the relative firing rate of the Up-states (from 0.86 ± 0.04 a.u. during control to 0.74 ± 0.27 a.u. with 1 µM *cis*-PAI) (**Fig. 2C, D)**. In summary, the most interesting differences between *trans*- and *cis*-PAI emerged between 100 nM and 300 nM, and were observed in the OF (Hz) and Up-states relative firing rate (a.u.) (**Fig. 2**). We focused on these conditions in order to photomodulate cortical SO using PAI.

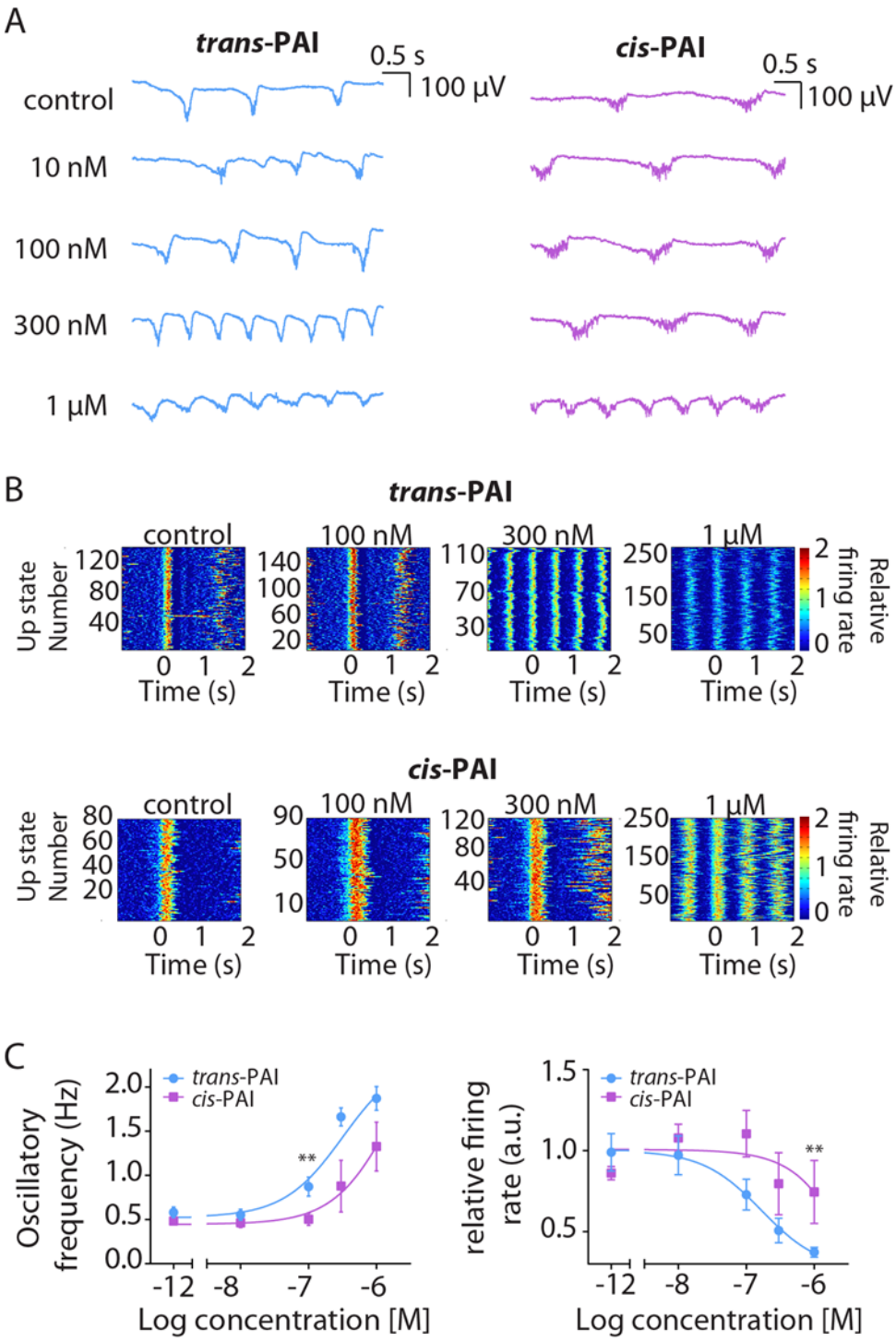

Figure 2: Effect of mAChRs activation by *trans*-PAI and *cis*-PAI on SO. (**A**) Raw LFP example recordings showing the different ability of *trans*- and *cis*-PAI to increasing the OF. (**B**) Raster plots showing the relative firing rate (color coded) under control conditions and different *trans*- and *cis*-PAI concentrations. (**C**) OF (Hz) and Relative firing rate (a.u.) of the two different PAI isomers, *trans*- (blue, n = 6) and *cis*-PAI (pink, n = 6) at different concentrations. (**p<0.01).

PAI effectively modulates cortical SO *in vitro*

Once the different oscillatory activity evoked by *cis*- and *trans*-PAI was quantified *in vitro* (**Fig.2**), we moved on to control SO activity with light in the same cortical slices (**Fig.3**). We took advantage of the thermal stability of both PAI forms to apply initially the inactive one (*cis*-PAI) at 200 nM in cortical slices (n = 15), in the absence of white light to avoid photoconversion to *trans*-PAI during the recordings.[23] As shown in **Fig.2**, 200 nM *cis*-PAI evoked minor changes in OF (from 0.53 ± 0.04 Hz in control conditions to 1.04 ± 0.14 Hz with *cis*-PAI), and no significant effects in the relative firing rate of the Up-states (from 0.98 ± 0.09 a.u. in the control to 0.86 ± 0.10 a.u. with *cis*-PAI) (**Fig. 3**). Subsequent illumination of the slices with white light produced a robust increase in OF (from 0.53 ± 0.04 Hz in the control to 1.68 ± 0.13 upon illumination), a decrease in relative firing rate of the Up-states (control: 0.98 ± 0.09 a.u.; white light: 0.52 ± 0.06 a.u.), and an increment of the power of delta (1-4 Hz) and theta (4-7 Hz) bands after light activation of PAI (*trans*) (**Fig. 3**). These changes are similar to the effects of adding Iperoxo to the bath (**Fig. 1**), and in agreement with PAI photoconversion to the active form (*trans*). The modification in cortical activity was not reversible with 365 nm light (to isomerize PAI to the *cis* form *in situ*), due either to the irreversibility of muscarinic stimulation in the absence of BF afferents and other circuit components in brain slices, or to neuronal damage produced by UV light.

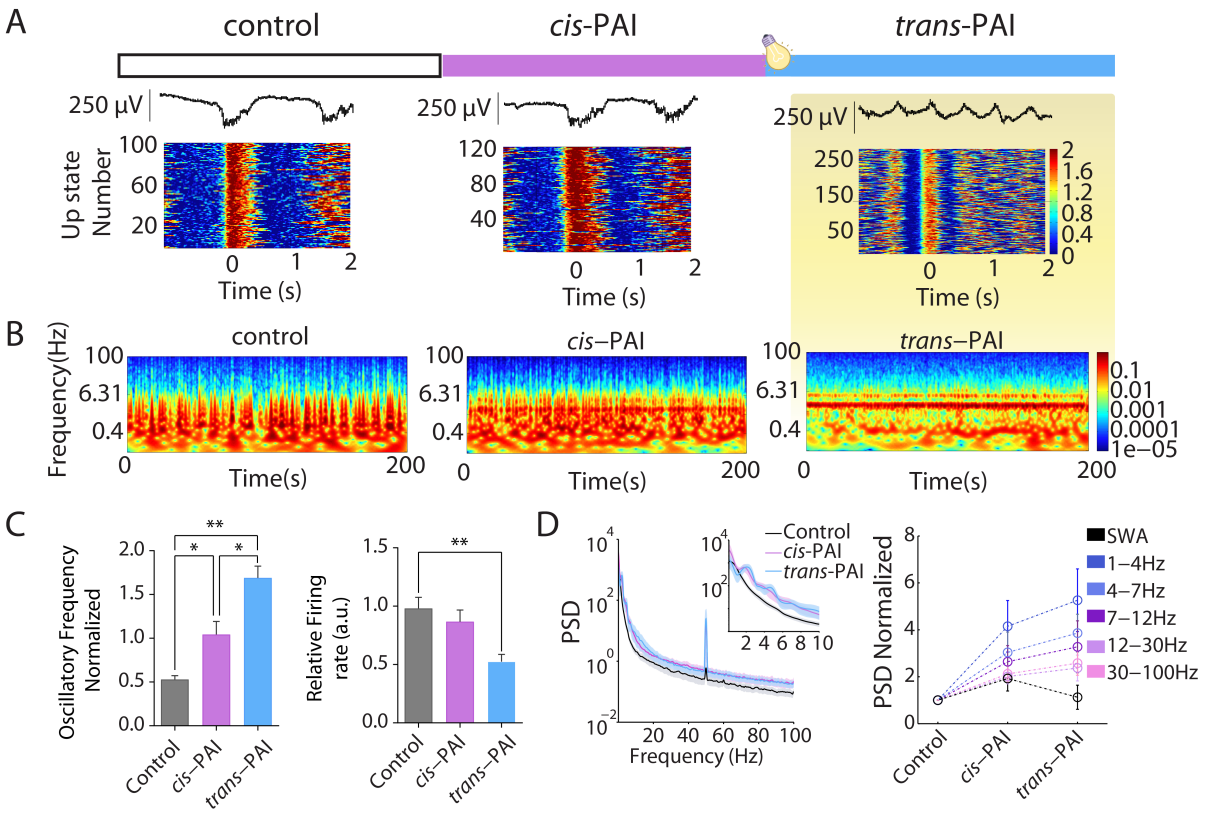

Figure 3: Modulation of brain waves in vitro using PAI, a light-regulated ligand. (**A**) Representative Local Field Potential traces (top) and raster plots of relative firing rate under control conditions, 200 nM of *cis*-PAI and 200 nM *trans*-PAI after light activation (n = 15) (bottom). (**B**) Representative spectrogram under control condition, 200 nM of *cis*-PAI and 200 nM *trans*-PAI after light activation. (**C**) OF (Hz) and relative firing rate of the Up-states (a.u.) at 200 nM PAI after pre-irradiation at 365 nm (*cis*-PAI), and photoswitching with white light (*trans*-PAI). (**D**) Averaged Power Spectral Density (PSD) under control conditions, 200 nM of *cis*-PAI and 200 nM *trans*-PAI after white light activation (color code). *p<0.0001 and **p<0.00001.

PAI can modulate brain wave activity with light *in vivo*

Having established the unique ability of PAI to alter cortical oscillatory activity with light in slices, we aimed at photocontrolling brain state transitions *in vivo*. Cortical brain waves were recorded in C57BL6/JR mice (n = 4) with a tungsten electrode inserted through a craniotomy that also enabled drug application and brain illumination (see Methods). Initially, we induced deep anesthesia in the animals, a state that is known to reproduce the slow wave sleep state,[25,26,41] and which is characterized by the generation of cortical SO similar to the slow frequency waves observed in our experiments in slices under control conditions (**Fig.1-3**).[6] Such SO activity in anesthetized mice was recorded for 500 s under white light illumination of the brain, and the characteristic parameters obtained (OF 0.64 ± 0.06 Hz, relative firing rate 0.83 ± 0.23 a.u.) were taken as the control condition *in vivo*. As the dose-response curves of *cis*- and *trans*-PAI could be different from the *in vitro* conditions (**Fig. 2**), we tested two different concentrations, 200 nM and 1 µM. 100 µL of 200 nM *cis*-PAI solution were initially applied to the brain surface, and the activity was recorded for another 500 s in the absence of white light, to avoid *cis* to *trans* photoisomerization of PAI. The frequency of the cortical oscillatory activity was not significantly altered by *cis*-PAI (0.61 ± 0.06 Hz), and caused a minor increase of the relative firing rate (1.02 ± 0.31 a.u.). Subsequently, we illuminated the brain using white light in the proximity of the tungsten electrode, in order to isomerize PAI to its active form (*trans*), and recorded the activity for another 500 s . An increase in OF to 0.76 ± 0.1 Hz was observed under white light illumination, without changes in the relative firing rate (1.04 ± 0.27 a.u.). Applying a higher concentration of *cis*-PAI (1 µM) slightly reduced the OF to 0.61 ± 0.1 without affecting the relative firing rate (0.99 ± 0.27 a.u.), and produced stronger effects on the cortical activity with light: the OF rose to 0.83 ± 0.06 Hz and the relative firing rate decreased to 0.86 ± 0.19 a.u. (**Fig. 4**). This allowed repeating twice the photocontrol of cortical activity by subsequent application of 1 µM *cis*-PAI and photoconversion to *trans*-PAI.

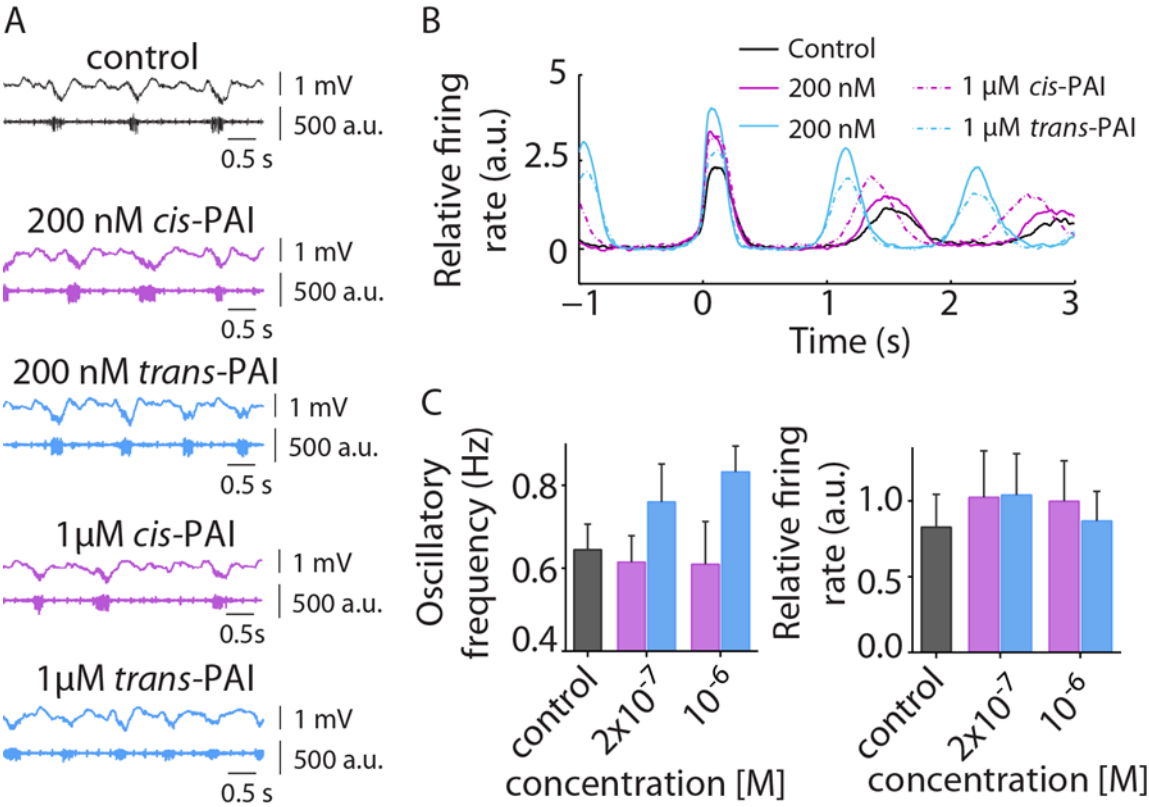

Figure 4: *In vivo* photomodulation of brain waves. (**A**) Representative raw traces of LFP (top) and Multiunit Activity (bottom), showing the differences in OF and relative firing rate between the control, 200 nM and 1 µM *cis*-PAI

(pre-irradiated at 365 nm) and photoswitching with white light (*trans*-PAI). (**B**) Representative examples of the waveform average of the MUA signal aligned at the Down-to-Up state transition under control, *cis*-PAI and *trans*-PAI at different concentrations (see legend). (**C**) Quantification of OF (Hz) and relative firing rate (Hz) at different concentrations.

DISCUSSION

Different brain states are associated with distinct behaviors. In order to investigate the causality between them, behavioral outcomes must be correlated with the spontaneous and evoked activity in the cortical network. Thus, understanding the mechanisms of brain and behavioral state transitions requires new techniques to manipulate neuronal activity.[1] They must enable the activation and inhibition of specific brain areas and neuronal circuits defined by several complementary criteria, namely electrical stimulation in selected regions, and photomanipulation that is cell-specific, or neurotransmitter-specific (using optogenetic and photopharmacology, respectively).

Modulation of brain waves is also therapeutically useful to treat CNS diseases, as shown by pioneering techniques to control cortical activity noninvasively based on electromagnetic stimulation.[42,43] Transcranial current stimulation enhances motor learning capacity in humans by cross-modulating the oscillatory neural activity (alpha and beta frequencies) in the motor cortex.[44–48] Transcranial magnetic stimulation can normalize excessive gamma oscillations in the prefrontal cortex, and restore cognitive performance in patients with schizophrenia, Alzheimer's and Parkinson's diseases,[49,50] and anxiety disorders.[51,52] However, the physiological mechanisms of brain wave modulation are not known, and they are essential to improve its spatiotemporal and spectral performance, both for fundamental and therapeutic purposes.[53]

Optogenetics[54,55] has emerged as an alternative to controlling brain waves with electromagnetic fields: photocontrolling the release of ACh, which strongly modulates the transitions between different brain states,[9,12] is possible by overexpressing photosensitive proteins in cholinergic neurons of mice neocortex.[10,56,57] However, genetic manipulation is required in this approach, and our light-dependent cholinergic muscarinic ligand is so far the only way to directly photomodulate cholinergic pathways in intact tissue. We first studied the effect of the superagonist Iperoxo[37] on isolated cortical slices (Fig. 1) in order to demonstrate that deep-sleep brain states can be controlled by selectively manipulating muscarinic receptors at their physiological location and context. The oscillatory frequency of the network was greatly increased already at 100 nM Iperoxo, and lead to periods of seizure-like discharges, in agreement with previous studies performed by knockout mice and pilocarpine[39,40] in which pathologic activation of muscarinic acetylcholine receptors induced seizures. Photocontrol of muscarinic signaling was subsequently achieved *in vitro* and *in vivo* with the photochromic iperoxo derivative PAI,[23] which is targeted allosterically at M2 subtype receptors (**Fig. 2-4**). In particular, PAI is a dualsteric ligand displaying full agonism, which is probably important to achieve effective photocontrol in slices, where axons from cholinergic afferents have been cut and the concentration of ACh can be assumed to be zero due to the degradation by extracellular esterases. M2 mAChRs are involved in several CNS diseases like major depressive[22,58] and bipolar disorders,[22,59] Parkinson's[22,60,61] and Alzheimer´s[22,61,62] diseases, but also in alcohol, smoking and drug dependence.[22,63,64] These disorders are thus susceptible to drug-based photomodulation *in vivo* without requiring genetic manipulation. Although PAI cannot cross the blood-brain barrier due to its charge, and its safety profile has not been systematically characterized, it is less likely to trigger immune reactions and mutagenesis than microbial opsins.

In summary, the manipulation of brain state transitions, by means of photocontrolling the frequency of cortical oscillations, has been achieved with a photoswitchable dualsteric agonist of M2 mAChRs. This result opens the way to (1) dissecting the spatiotemporal distribution and pharmacology of brain states, namely how they depend on agonists, antagonists, and modulators of the different muscarinic subtypes expressed in the CNS, and (2) investigating the neuronal dynamics that regulate brain state transitions in the cortical surface and beyond. In particular, two-photon stimulation of PAI using pulsed infrared light[23] offers the promise of subcellular resolution in three dimensions, as recently demonstrated with endogenous $mGlu_5$.[65] Compared to the local and often inhomogeneous expression patterns achieved with viral injections of optogenetic constructs, diffusible small molecules like PAI can be in principle applied to larger brain regions to control neuronal oscillations.[57] Thus, remote control of brain waves based on the photopharmacological manipulation of endogenous muscarinic receptors may reveal the complex 3D molecular signalling underlying brain states and their transitions, in order to link them with cognition and behavior in a diversity of wildtype organisms.

EXPERIMENTAL PROCEDURES

Slice Preparation

Twenty-five ferrets (4- to 6-month-old) were anesthetized with sodium pentobarbital (40 mg/kg) and decapitated. The entire forebrain was rapidly removed and placed in oxygenated cold (4–10 °C) bathing medium.[38] Ferrets were treated in accordance with protocols approved by the Animal Ethics Committee of the University of Barcelona, which comply with the European Union guidelines on protection of vertebrates used for experimentation (Directive 2010/63/EU of the European Parliament and the Council of 22 September 2010). Coronal slices (400 µm thick) from primary visual cortex (V1) were used.[66] To increase tissue viability we used a modification of the sucrose-substitution technique.[67] During slice preparation, the tissue was placed in a solution in which NaCl was replaced with sucrose while maintaining the same osmolarity. After preparation, the slices were placed in an interface-style recording chamber (Fine Sciences Tools, Foster City, CA, USA). During the first 30 min the cortical slices were superfused with an equal mixture in volume of the normal bathing medium, artificial cerebral spinal fluid (ACSF) and the sucrose-substituted solution. Following this, normal bathing medium was added to the recording chamber and the slices were superfused for 1–2 h; the normal bathing medium contained (in mM): NaCl, 126; KCl, 2.5; $MgSO_4$, 2; Na_2HPO_4, 1; $CaCl_2$, 2; $NaHCO_3$, 26; dextrose, 10; and was aerated with 95% O_2, 5% CO_2 to a final pH of 7.4. Then, a modified slice solution was used throughout the rest of the experiment; it had the same ionic composition except for different levels of the following (in mM): KCl, 4; $MgSO_4$, 1; and $CaCl_2$, 1.[38] Bath temperature was maintained at 34–36 °C.

Drug application and photostimulation in brain slices

Iperoxo and PAI, both prepared as previously reported from commercially available starting materials,[23] were bath-applied at the concentrations range of 1 nM to 100 nM for Iperoxo and 10 nM to 1 uM for PAI, as it is mention in Results section. We usually waited more than 1000 s after the application of the drug in order to let it act and to obtain a stable pattern of electrical activity, and to ensure a stable concentration in the bath. PAI effectively photomodulates the activity of M2 receptors *in vitro* and *in vivo*: in its dark-adapted state (*trans* form) behaves as a strong M2 agonist, then upon illumination with UV light (365 nm), PAI switches to its off-state (*cis* form). PAI can be switched back to its on-state with blue or white light, or using 2 photon excitation with pulsed NIR light.[23] The high thermal stability of PAI inactive form (*cis* isomer) allows administering the inactive drug and subsequently activating M2 receptors in the target region with white

light.[23] We first investigated the efficacy of PAI in cortical neuronal circuits *in vitro* by obtaining the dose-response curves of *trans*- and *cis*-PAI solutions applied separately. The more active PAI isomer (*trans*) was tested by applying its dark-adapted form (87 % of *trans*-PAI), and *cis*-PAI was obtained by illuminating 1 mM stock solutions with 365 nm light for 10 min (73% of *cis*-PAI).[23] Increasing concentrations of both *trans*- and *cis*-PAI (10 nM, 100 nM, 300 nM and 1 µM) were bath applied in order to build up the dose-response curves.

LFP recording and data analysis from *in vitro* recordings

LFP recordings started after allowing at least 2 h of recovery of the slices. Extracellular multiple unit recordings were obtained with flexible arrays of 16 electrodes arranged in columns as in Figure (**Figure 1A**). The multielectrode array (MEA) covered most of the area occupied by a cortical slice. It consisted of 6 groups of electrodes positioned to record electrophysiological activity from superficial and from deep cortical layers (692 µm apart) and from what should correspond to 3 different cortical columns (1500 µm apart). The unfiltered field potential (raw signal) was acquired at 10 kHz with a Multichannel System Amplifier (MCS, Reutlingen, Germany) and digitized with a 1401 CED acquisition board and Spike2 software (Cambridge Electronic Design, Cambridge, UK). The multiunit activity (MUA) was estimated as the power change in the Fourier components at high frequencies from the recorded LFP.[68] Up-state detection was performed by setting a threshold in the log(MUA) time series as previously described to quantify frequency of the slow oscillations.[6,69] Relative firing rate (FR) of the Up-states were quantified from the transformed log(MUA) signal as mean of absolute value of log(MUA). To study the variability of power spectral densities (PSD) of the local field potential, we used Welch's method with 50% overlapped Hamming window with a resolution of 1 Hz. All off-line estimates and analyses were implemented in MATLAB (The MathWorks Inc., Natick, MA, USA). All variables in the experimental conditions were compared with the control (no chemical added) condition.

The *in vivo* preparation

Cortical electrophysiology experiments were carried out in 2-3 months old C57BL6/JR mice (n = 4) in accordance with the European Union Directive 2010/63/EU and approved by the local ethical committee. Mice were kept under standard conditions (room temperature, 12:12-h light-dark cycle, lights on at 08:00 a.m). Anesthesia was induced by intraperitoneal injection of ketamine (30 mg/kg) and medetomidine (100 mg/kg). After this procedure, the mouse was placed in a stereotaxic frame, and air was enriched with oxygen. Body temperature was maintained at 37°C throughout the experiment.[6] Slow and fast rhythms generated in the cerebral cortex of the anesthetized mouse.[70] Slow and fast neocortical oscillations in the senescence-accelerated mouse model SAMP8. Frontiers in aging neuroscience, 9, 141). Craniotomy was made in each mouse: AP −2.5 mm, L 1.5 mm (primary visual cortex, V1).[71] Cortical recordings were obtained from infragranular layers with 1–2 MΩ single tungsten electrode insulated with a plastic coating except for the tip (FHC, Bowdoin, ME, USA). Spontaneous local field potential (LFP) recordings from V1 area provide information about the local neuronal population activity—within 250 µm.[72] MUA estimation, Up-state detection and quantification of relative FR was performed as previously described. All these parameters were used to compare spontaneous activity during anesthesia (control), after application of the pre-illuminated, inactive drug form (*cis*-PAI) and application of white light to activate the drug (*trans*-PAI). *Cis*-PAI was locally delivered to the cerebral cortex surface and activity was recorded while applying a commercial red filter on the white light source to avoid the activation of the drug. The uncovered brain was illuminated with a white light source (Photonic Optics™ Optics Cold Light Source LED F1) in order to *in situ* activate the drug (*trans*-PAI). The electrophysiological signal was amplified with a multichannel system (Multi Channel

Systems), digitized at 20 kHz with a CED acquisition board and acquired with Spike 2 software (Cambridge Electronic Design) unfiltered.[70]

Statistical analysis for slice experiments

Both *in vitro* and *in vivo* oscillatory frequency (OF) are reported as mean ± SEM. Measurements under different conditions were compared using the Friedman test and the Wilcoxon post-hoc tests corrected for multiple comparisons.[73]

References

1. Andalman, A. S. *et al.* Neuronal Dynamics Regulating Brain and Behavioral State Transitions. *Cell* **177**, 970-985.e20 (2019).
2. Wang, S. *et al.* Neurons in the human amygdala selective for perceived emotion. *Proc. Natl. Acad. Sci. U. S. A.* **111**, E3110-9 (2014).
3. Krehbiel, D., Bartel, B., Dirks, M. & Wiens, W. Behavior and brain neurotransmitters: Correlations in different strains of mice. *Behav. Neural Biol.* **46**, 30–45 (1986).
4. Hanin, I. Central neurotransmitter function and its behavioral correlates in man. *Environ. Health Perspect.* **26**, 135–141 (1978).
5. Peyrache, A. *et al.* Spatiotemporal dynamics of neocortical excitation and inhibition during human sleep. *Proc. Natl. Acad. Sci. U. S. A.* **109**, 1731–6 (2012).
6. Ruiz-Mejias, M., Ciria-Suarez, L., Mattia, M. & Sanchez-Vives, M. V. Slow and fast rhythms generated in the cerebral cortex of the anesthetized mouse. *J. Neurophysiol.* **106**, 2910–21 (2011).
7. Sanchez-Vives, M. V & Mattia, M. Slow wave activity as the default mode of the cerebral cortex. *Arch. Ital. Biol.* **152**, 147–55
8. Muller, L., Reynaud, A., Chavane, F. & Destexhe, A. The stimulus-evoked population response in visual cortex of awake monkey is a propagating wave. *Nat. Commun.* **5**, 3675 (2014).
9. Lee, S.-H. & Dan, Y. Neuromodulation of Brain States. *Neuron* **76**, 209–222 (2012).
10. Pinto, L. *et al.* Fast modulation of visual perception by basal forebrain cholinergic neurons. *Nat. Neurosci.* **16**, 1857–1863 (2013).
11. Ramaswamy, S., Colangelo, C. & Markram, H. Data-Driven Modeling of Cholinergic Modulation of Neural Microcircuits: Bridging Neurons, Synapses and Network Activity. *Front. Neural Circuits* **12**, 77 (2018).
12. Hasselmo, M. E. & Sarter, M. Modes and Models of Forebrain Cholinergic Neuromodulation of Cognition. *Neuropsychopharmacology* **36**, 52–73 (2011).
13. Buzsàki, G. & Gage, F. H. The cholinergic nucleus basalis: a key structure in neocortical arousal. *EXS* **57**, 159–71 (1989).
14. Herrero, J. L. *et al.* Acetylcholine contributes through muscarinic receptors to attentional modulation in V1. *Nature* **454**, 1110–1114 (2008).
15. Conner, J. M., Culberson, A., Packowski, C., Chiba, A. A. & Tuszynski, M. H. Lesions of the Basal forebrain cholinergic system impair task acquisition and abolish cortical plasticity associated with motor skill learning. *Neuron* **38**, 819–29 (2003).

16. Kilgard, M. Cholinergic modulation of skill learning and plasticity. *Neuron* **38**, 678–80 (2003).

17. Ramanathan, D., Tuszynski, M. H. & Conner, J. M. The Basal Forebrain Cholinergic System Is Required Specifically for Behaviorally Mediated Cortical Map Plasticity. *J. Neurosci.* **29**, 5992–6000 (2009).

18. Winkler, J., Suhr, S. T., Gage, F. H., Thal, L. J. & Fisher, L. J. Essential role of neocortical acetylcholine in spatial memory. *Nature* **375**, 484–487 (1995).

19. Berg, R. W., Friedman, B., Schroeder, L. F. & Kleinfeld, D. Activation of Nucleus Basalis Facilitates Cortical Control of a Brain Stem Motor Program. *J. Neurophysiol.* **94**, 699–711 (2005).

20. Kilgard, M. P. & Merzenich, M. M. Cortical Map Reorganization Enabled by Nucleus Basalis Activity. *Science (80-.).* **279**, 1714–1718 (1998).

21. Henny, P. & Jones, B. E. Projections from basal forebrain to prefrontal cortex comprise cholinergic, GABAergic and glutamatergic inputs to pyramidal cells or interneurons. *Eur. J. Neurosci.* **27**, 654–670 (2008).

22. Scarr, E. Muscarinic Receptors: Their Roles in Disorders of the Central Nervous System and Potential as Therapeutic Targets. *CNS Neurosci. Ther.* **18**, 369–379 (2012).

23. Riefolo, F. *et al.* Optical Control of Cardiac Function with a Photoswitchable Muscarinic Agonist. *J. Am. Chem. Soc.* **141**, 7628–7636 (2019).

24. McCormick, D. A. Cellular mechanisms underlying cholinergic and noradrenergic modulation of neuronal firing mode in the cat and guinea pig dorsal lateral geniculate nucleus. *J. Neurosci.* **12**, 278–89 (1992).

25. Steriade, M., Amzica, F. & Nunez, A. Cholinergic and noradrenergic modulation of the slow (approximately 0.3 Hz) oscillation in neocortical cells. *J. Neurophysiol.* **70**, 1385–1400 (1993).

26. Steriade, M. Cholinergic blockage of network- and intrinsically generated slow oscillations promotes waking and REM sleep activity patterns in thalamic and cortical neurons. *Prog. Brain Res.* **98**, 345–55 (1993).

27. Jacobs, S. E. & Juliano, S. L. The impact of basal forebrain lesions on the ability of rats to perform a sensory discrimination task involving barrel cortex. *J. Neurosci.* **15**, 1099–109 (1995).

28. Xiang, Z., Huguenard, J. R. & Prince, D. A. Cholinergic switching within neocortical inhibitory networks. *Science* **281**, 985–8 (1998).

29. Picciotto, M. R., Higley, M. J. & Mineur, Y. S. Acetylcholine as a neuromodulator: cholinergic signaling shapes nervous system function and behavior. *Neuron* **76**, 116–29 (2012).

30. Zagha, E. & McCormick, D. A. Neural control of brain state. *Curr. Opin. Neurobiol.* **29**, 178–86 (2014).

31. Kuczewski, N., Aztiria, E., Gautam, D., Wess, J. & Domenici, L. Acetylcholine modulates cortical synaptic transmission via different muscarinic receptors, as studied with receptor knockout mice. *J. Physiol.* **566**, 907–919 (2005).

32. Wester, J. C. & Contreras, D. Differential modulation of spontaneous and evoked thalamocortical network activity by acetylcholine level in vitro. *J. Neurosci.* **33**, 17951–66 (2013).

33. Compte, A. *et al.* Spontaneous High-Frequency (10-80 Hz) Oscillations during Up States in the Cerebral Cortex In Vitro. *J. Neurosci.* **28**, 13828–13844 (2008).

34. Schmidt, S. L., Chew, E. Y., Bennett, D. V., Hammad, M. A. & Fröhlich, F. Differential effects of cholinergic and noradrenergic neuromodulation on spontaneous cortical network dynamics. *Neuropharmacology* **72**, 259–273 (2013).

35. Castro-Alamancos, M. A. & Gulati, T. Neuromodulators produce distinct activated states in neocortex. *J. Neurosci.* **34**, 12353–67 (2014).

36. McCormick, D. A. & Williamson, A. Convergence and divergence of neurotransmitter action in human cerebral cortex. *Proc. Natl. Acad. Sci. U. S. A.* **86**, 8098–102 (1989).

37. Barocelli, E. *et al.* New analogues of oxotremorine and oxotremorine-M: estimation of their in vitro affinity and efficacy at muscarinic receptor subtypes. *Life Sci.* **67**, 717–23 (2000).

38. Mattia, M. & Sanchez-Vives, M. V. Exploring the spectrum of dynamical regimes and timescales in spontaneous cortical activity. *Cogn. Neurodyn.* **6**, 239–250 (2012).

39. Yi, F. *et al.* Muscarinic excitation of parvalbumin-positive interneurons contributes to the severity of pilocarpine-induced seizures. *Epilepsia* **56**, 297–309 (2015).

40. Hamilton, S. E. *et al.* Disruption of the m1 receptor gene ablates muscarinic receptor-dependent M current regulation and seizure activity in mice. *Proc. Natl. Acad. Sci.* **94**, 13311–13316 (1997).

41. Steriade, M., Contreras, D., Curró Dossi, R. & Nuñez, A. The slow (< 1 Hz) oscillation in reticular thalamic and thalamocortical neurons: scenario of sleep rhythm generation in interacting thalamic and neocortical networks. *J. Neurosci.* **13**, 3284–99 (1993).

42. Antal, A. *et al.* Comparatively weak after-effects of transcranial alternating current stimulation (tACS) on cortical excitability in humans. *Brain Stimul.* **1**, 97–105 (2008).

43. Terney, D., Chaieb, L., Moliadze, V., Antal, A. & Paulus, W. Increasing Human Brain Excitability by Transcranial High-Frequency Random Noise Stimulation. *J. Neurosci.* **28**, 14147–14155 (2008).

44. Sugata, H. *et al.* Modulation of Motor Learning Capacity by Transcranial Alternating Current Stimulation. *Neuroscience* **391**, 131–139 (2018).

45. Pollok, B., Boysen, A.-C. & Krause, V. The effect of transcranial alternating current stimulation (tACS) at alpha and beta frequency on motor learning. *Behav. Brain Res.* **293**, 234–240 (2015).

46. Joundi, R. A., Jenkinson, N., Brittain, J.-S., Aziz, T. Z. & Brown, P. Driving Oscillatory Activity in the Human Cortex Enhances Motor Performance. *Curr. Biol.* **22**, 403–407 (2012).

47. Pogosyan, A., Gaynor, L. D., Eusebio, A. & Brown, P. Boosting Cortical Activity at Beta-Band Frequencies Slows Movement in Humans. *Curr. Biol.* **19**, 1637–1641 (2009).

48. Moisa, M., Polania, R., Grueschow, M. & Ruff, C. C. Brain Network Mechanisms Underlying Motor Enhancement by Transcranial Entrainment of Gamma Oscillations. *J. Neurosci.* **36**, 12053–12065 (2016).

49. Pereira, L. S., Müller, V. T., da Mota Gomes, M., Rotenberg, A. & Fregni, F. Safety of repetitive transcranial magnetic stimulation in patients with epilepsy: A systematic review. *Epilepsy Behav.* **57**, 167–176 (2016).

50. Lefaucheur, J.-P. Treatment of Parkinson's disease by cortical stimulation. *Expert Rev. Neurother.* **9**, 1755–71 (2009).

51. Xiao, Z., Li, C. & Wang, J. Repetitive transcranial magnetic stimulation (rTMS) for panic disorder. in *Cochrane Database of Systematic Reviews* (ed. Wang, J.) (John Wiley & Sons, Ltd, 2011). doi:10.1002/14651858.CD009083

52. Lefaucheur, J.-P. *et al.* Evidence-based guidelines on the therapeutic use of repetitive transcranial magnetic stimulation (rTMS). *Clin. Neurophysiol.* **125**, 2150–2206 (2014).

53. Paulus, W. Transcranial brain stimulation: potential and limitations. *e-Neuroforum* **5**, 29–36 (2014).

54. Cardin, J. A. *et al.* Driving fast-spiking cells induces gamma rhythm and controls sensory responses. *Nature* **459**, 663–667 (2009).

55. Sohal, V. S., Zhang, F., Yizhar, O. & Deisseroth, K. Parvalbumin neurons and gamma rhythms enhance cortical circuit performance. *Nature* **459**, 698–702 (2009).

56. Zucca, S., Pasquale, V., Lagomarsino de Leon Roig, P., Panzeri, S. & Fellin, T. Thalamic Drive of Cortical Parvalbumin-Positive Interneurons during Down States in Anesthetized Mice. *Curr. Biol.* **29**, 1481-1490.e6 (2019).

57. Zucca, S. *et al.* An inhibitory gate for state transition in cortex. *Elife* **6**, (2017).

58. Gibbons, A. S., Scarr, E., McLean, C., Sundram, S. & Dean, B. Decreased muscarinic receptor binding in the frontal cortex of bipolar disorder and major depressive disorder subjects. *J. Affect. Disord.* **116**, 184–91 (2009).

59. Cannon, D. M. *et al.* Reduced Muscarinic Type 2 Receptor Binding in Subjects With Bipolar Disorder. *Arch. Gen. Psychiatry* **63**, 741 (2006).

60. Warren, N. M., Piggott, M. A., Lees, A. J. & Burn, D. J. The basal ganglia cholinergic neurochemistry of progressive supranuclear palsy and other neurodegenerative diseases. *J. Neurol. Neurosurg. Psychiatry* **78**, 571 (2007).

61. Piggott, M. A. *et al.* Muscarinic receptors in basal ganglia in dementia with Lewy bodies, Parkinson's disease and Alzheimer's disease. *J. Chem. Neuroanat.* **25**, 161–73 (2003).

62. Quirion, R. Cholinergic markers in Alzheimer disease and the autoregulation of acetylcholine release. *J. Psychiatry Neurosci.* **18**, 226–34 (1993).

63. Dick, D. M. *et al.* Alcohol dependence with comorbid drug dependence: genetic and phenotypic associations suggest a more severe form of the disorder with stronger genetic contribution to risk. *Addiction* **102**, 1131–1139 (2007).

64. Mobascher, A. *et al.* Association of a variant in the muscarinic acetylcholine receptor 2 gene (CHRM2) with nicotine addiction. *Am. J. Med. Genet. Part B Neuropsychiatr. Genet.* **153B**, 684–690 (2010).

65. Pittolo, S. *et al.* Reversible silencing of endogenous receptors in intact brain tissue using 2-photon pharmacology. *Proc. Natl. Acad. Sci.* **116**, 13680–13689 (2019).

66. Krimer, L. S. & Goldman-Rakic, P. S. Prefrontal microcircuits: membrane properties and excitatory input of local, medium, and wide arbor interneurons. *J. Neurosci.* **21**, 3788–96 (2001).

67. Aghajanian, G. K. & Rasmussen, K. Intracellular studies in the facial nucleus illustrating a simple new method for obtaining viable motoneurons in adult rat brain slices. *Synapse* **3**, 331–338 (1989).

68. Mattia, M. & Del Giudice, P. Population dynamics of interacting spiking neurons. *Phys. Rev. E* **66**, 051917 (2002).

69. Sanchez-Vives, M. V *et al.* Inhibitory modulation of cortical up states. *J. Neurophysiol.* **104**, 1314–24 (2010).

70. Castano-Prat, P., Perez-Zabalza, M., Perez-Mendez, L., Escorihuela, R. M. & Sanchez-Vives, M. V. Slow and Fast Neocortical Oscillations in the Senescence-Accelerated Mouse Model SAMP8. *Front. Aging Neurosci.* **9**, 141 (2017).

71. Golmohammadi, M. G. *et al.* Comparative Analysis of the Frequency and Distribution of Stem and Progenitor Cells in the Adult Mouse Brain. *Stem Cells* **26**, 979–987 (2008).

72. Katzner, S. *et al.* Local Origin of Field Potentials in Visual Cortex. *Neuron* **61**, 35–41 (2009).

73. Benjamini, Y. & Hochberg, Y. Controlling the False Discovery Rate: A Practical and Powerful Approach to Multiple Testing. *Journal of the Royal Statistical Society. Series B (Methodological)* **57**, 289–300 (1995).